Environmental Earth Sciences (2018) 77:167
https://doi.org/10.1007/s12665-018-7340-7

THEMATIC ISSUE

# Building stones used in the architectural heritage of Morelia (México): quarries location, rock durability and stone compatibility in the monument

J. Martínez-Martínez[1,2] · A. Pola[3] · L. García-Sánchez[4] · G. Reyes Agustin[5] · L. S. Osorio Ocampo[4] · J. L. Macías Vázquez[4] · J. Robles-Camacho[6]

Received: 31 October 2017 / Accepted: 14 February 2018 / Published online: 24 February 2018


## Abstract
Four different rocks have been used in the architectural heritage of Morelia city (Michoacán state, México). Piedra Vieja (PV) is the original building rock whilst Tlalpujahua, Cointzio and Jabalina stones (TL, CO and JA, respectively) are the replacement varieties used in the restoration works during the last decades. All of them correspond to rhyolitic ignimbrites quarried close to Morelia. The new varieties were selected exclusively after aesthetical similarity, and no petrophysical criterion was considered. In this paper, a deep analysis of the weathering process of these rocks during wet–dry and salt crystallization cycles is carried out. Rock decay is defined in terms of linearity and homogeneity: JA and TL show nonlinear decay mode and heterogeneous behaviours, whilst samples of CO and PV weather after linear and homogeneous modes. Moreover, each rock variety shows different decay patterns, such as differential erosion (PV and TL), fractures (TL), scaling (JA) and granular disintegration (CO). All these obtained results are discussed according to: (1) petrographic factors; (2) hydric and mechanical properties; and (3) the partial effective pressures reached inside the porous system of each rock during salt crystallization. Finally, a review about the quality of previously published durability estimators is carried out. In general terms, results reveal that theoretical estimators best fit the visual weathering suffered by the rocks than its mass loss. Concluding this paper, a petrophysical and aesthetical evaluation of the compatibility between both original and replacement building stones used in the architectural heritage of Morelia is carried out in order to offer technical recommendations for future restoration works. CO ignimbrite offers the highest chromatic compatibility with the original building rock (PV), but its durability is extraordinarily low and consequently its use is not recommended. JA and TL are advisable replacement stones, although from a petrophysical point of view, TL results the most convenient. These results highlight the importance of carrying out the selection of building stones for restoration works according to petrophysical criteria, instead of using exclusively an aesthetic valuation.

**Keywords** Ignimbrite · Salt weathering · Wet–dry test · Porous media · Stone compatibility

This article is part of a Topical Collection in Environmental Earth Sciences on "Stone in the Architectural Heritage: from quarry to monuments – environment, exploitation, properties and durability", guest edited by Siegfried Siegesmund, Luís Sousa, and Rubén Alfonso López-Doncel.

✉ J. Martínez-Martínez
javier.martinez@igme.es

1 Facultad de Ciencias, Universidad de Alicante, Alicante, Spain

2 Spanish Geological Survey (Instituto Geológico y Minero de España, IGME), Madrid, Spain

3 Unidad Morelia, Geociencias, Escuela Nacional de Estudios Superiores, Universidad Nacional Autónoma de México, Morelia, Mexico

4 Instituto de Geofísica, Universidad Nacional Autónoma de México - Campus Morelia, Morelia, Mexico

5 Instituto de Investigaciones en Ciencias de la Tierra, Universidad Michoacana de San Nicolás de Hidalgo, Morelia, Mexico

6 Laboratorio de Arqueometría del Occidente-Centro INAH Michoacán, Instituto Nacional de Antropología e Historia, Morelia, Mexico

## Introduction

Ignimbrite-type rocks have long been widely used as natural building materials due to their availability, their relatively low weight, aesthetic properties and ease of processing. The widespread use of this kind of rock in cultural heritage justifies the plenty of researches and publications focused on their petrophysical properties and decay resistance (Topal and Doyuran 1998; Ulusoy 2007; Zedef et al. 2007; Korkanç 2013; López-Doncel et al. 2013; Özbek 2014; Yavuz et al. 2015), weathering processes acting on this kind of rocks (Alonso and Martínez 2003; Ostroumov et al. 2003; Chen et al. 2004; Wedekind et al. 2013; López-Moreno et al. 2014; Di Benedetto et al. 2015; Özvan et al. 2015; López-Doncel et al. 2016), as well as the effectiveness of restoration

**Fig. 1** Building stones used in the architectural heritage of Morelia: Piedra Vieja (**a**–**c**); Cointzio (**d**–**g**) and Jamaica (**h**–**j**). Different decay patterns are showed: efflorescences (**a**, **f**), differential erosion and scaling (**b**, **c**), pitting and sanding (**e**), alveolization (**f**, **g**), scaling (**h**, **j**) and flaking (**i**)

treatments applied on them (Penide et al. 2013; La Russa et al. 2014).

This study is focused on the ignimbrites used as building stones in the architectural heritage of Morelia (Michoacán state, México) (Fig. 1). One of the most singular aspects of this colonial city (included in the list of world heritage sites by UNESCO in 1991) is the exclusive use of a local pink stone, giving a high aesthetical homogeneity to the historic city. Consequently, one of the most restrictive criteria during the restoration works of buildings is the prevalence of its aesthetical homogeneity. That fact limits the possibilities for selecting the replacement rock, being mandatory the use of pink stones. The original rock employed in the architectural heritage of Morelia is a rhyolitic ignimbrite, named "Piedra Vieja". Historical quarries of this original stone are located in the vicinity of the old city and nowadays are under the new buildings of the urban expansion area. As a consequence, it is impossible to obtain new rock volume from the old historic quarries for restoration works and, therefore, different replacement stones must be chosen. Three different building rocks have been used during the last decades: Cointzio, Jamaica and Tlalpujahua stones (Fig. 2a, b).

The use of Cointzio, Tlalpujahua and Jamaica stones was exclusively justified in their similar colour to the original rock and their lithology (all of them are ignimbrites), but no other petrophysical criterion was considered. The use of inappropriate replacement stones can result in significant damage to the heritage as well as in the inefficiency of the restoration works. Because of this reason, the choice of the replacement stone should be appropriate in physical and aesthetic terms and, ideally, it should be of the same type as the original building stone, or the nearest possible equivalent (Pereira and Marker 2016). It is generally accepted that the main physical properties for stone compatibility are their hydro-mechanic behaviour in terms of such properties as water absorption, capillarity or mechanical strength, which are dependent, in turn, on the porous system of the rock (Andriani and Walsh 2003; Rozenbaum et al. 2008).

Rock durability is one of the most important aspects defining the quality of building materials for restoration

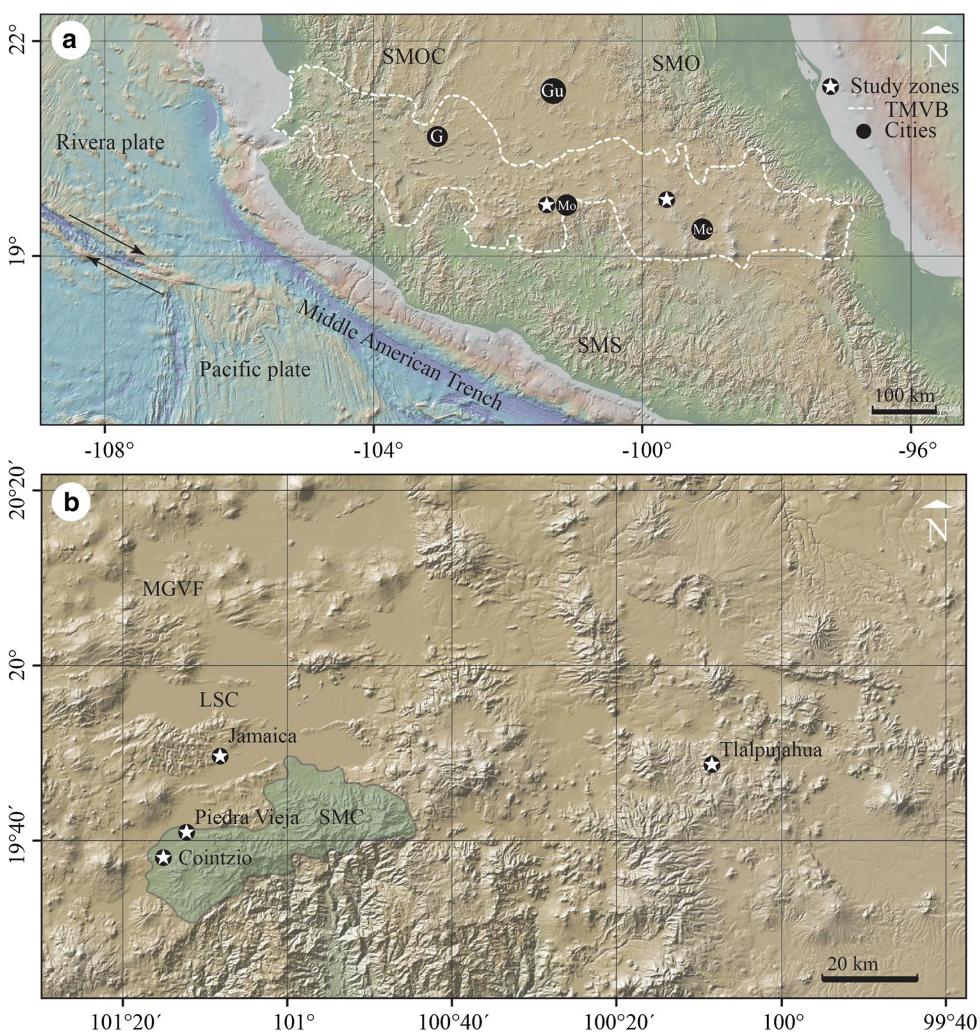


**Fig. 2** **a** Illustrative map of the central part of Mexico, including the trace of the TMVB, the most representative cities, as well as studied zone. Image was constructed by GeoMapApp free application of earth science exploration and visualization (http://www.geomapapp.org). **b** Localization map of the studies zones, including labels of the regional geological units. Abbreviations are: G, Guadalajara; Gu, Guanajuato; Mo, Morelia; Me, Mexico city; SMOC, Sierra Madre Occidental; SMO, Sierra Madre Oriental; SMS, Sierra Madre del Sur; MGVF, Michoacan Guanajuato volcanic field; LSC, Lacustrine sediments of Cuitzeo Lake; SMC, Sierra de Mil Cumbres

works as well as for new constructions. Many studies have been carried out using experimental laboratory simulations to assess stone durability produced by salt weathering, frost action and wetting and drying cycles. However, since durability tests are time-consuming, destructive and costly, attempts are also made to assess the durability of porous building materials by means of different indirect estimators. For this purpose, the hydromechanics properties of rocks have been employed in durability predictions as they control the rock susceptibility to weathering.

The aim of this study is to evaluate building stone behaviour during accelerated ageing, and to understand how the porous network controls the weathering process. Rock resistance to salt crystallization and wet–dry cycles are studied because they are considered the most aggressive mechanisms acting on this kind of rocks (Madsen and Müller-Vonmoos 1989; Columbu et al. 2014; Julia et al. 2014). The weathering patterns and forms that occur in selected ignimbrites are studied, and their behaviours due to salt crystallization are predicted from their pore size distribution and strength. Moreover, a review about the quality of published durability estimators is carried out. They are used for assessing the damages achieved by the studied rocks during the ageing tests. Finally, a petrophysical and aesthetical evaluation of the compatibility between both original and replacement building stones used in the architectural heritage of Morelia is carried out in order to offer technical recommendations for future restoration works.

## Geological setting and quarries location

According to previous studies, the geology of the Cuizeo and Morelia regions is composed by at least three different large units (e.g. Ferrari et al. 1994; Pradal and Robin 1994; Garduño-Monroy et al. 2001; Cisneros-Máximo 2015), described from older to younger as follows (Fig. 2a, b):

1. The Sierra de Mil Cumbres (SMC) (15–24 Ma) that consists of La Escalera and Atécuaro calderas, and the Indaparapeo, Garnica and Punhuato volcanic complexes made of different volcanic and volcaniclastic deposits (Gómez-Vasconcelos et al. 2015) (Fig. 2b);
2. Volcanoes of the Michoacán–Guanajuato volcanic field (MGVF) ($1.42 \pm 0.12$ to $0.33 \pm 0.04$ Ma) that in the region are represented by the Quinceo–Tetillas volcanoes, identified as the source of different volcanic materials (Gómez-Vasconcelos et al. 2015);
3. Lacustrine sediments of the Cuitzeo Lake (LSC) interbedded with fallout layers (Fig. 2b).

The Atécuaro caldera of the SMC is composed of several ignimbrite lithofacies related to the caldera collapse occurred ~ 16 Ma. The lithofacies consists of ignimbrites with different welding degrees. Particularly, the ignimbrite blocks used for the construction and restoration of the historical monuments of the Morelia city have been extracted from the Cointzio, Río Chiquito and Morelia downtown quarries, corresponding to the last and welded lithofacies (Ostroumov et al. 2003).

Piedra Vieja quarry is located in the northern part of Morelia downtown, all along Canteros street, within the Indias de San Juan antique neighbourhood (UTM *X*: 271197 *Y*: 2180748). These quarries include several outcrops restricted by the urban growth and entire composed by the upper part of a white to pink-violet welded ignimbrite lithofacies. The lateral, and proximal–distal changes of this upper part could be identified in several outcrops around Morelia city (e.g. Río Chiquito and Santa María outcrops). Particularly, this layer is characterized by different proportions of cm size deformed pumices and large content of lithics, supported by a fine-rich and very consolidated matrix composed prevalently by glass and lithics. With the petrographic description were observed crystals of quartz, plagioclase and biotite immersed in a matrix of glass and small crystals of plagioclase (Fig. 3PV-a to PV-c). It is notable in Fig. 3PV-b that the biotite presents dark brown rims.

Cointzio quarry is located 1 km to the north of the Cointzio dam, near the southern margin of the city of Morelia (UTM *X*: 263268; *Y*: 2173053). The general stratigraphy of the outcrop is composed of two different layers of ignimbrites, vertically differentiated by the degree of welding and the content and distribution of pumices and lithics. The lower level corresponds to a pink welded layer composed of mm-to-cm brown lithics and random distributed lenses of pumices with different sizes and internal structures. The upper part of the outcrop is composed of at least five white layers, vertically differentiated by the thickness, the degree of welding and the abundance of pumices fragments. The most representative layer of this upper part is 18 m thick, and it is welded and compacted with brittle zones. Large lithics and pumice fragments (< 15 cm), spherulites (< 2 cm), quartz and feldspar in the matrix are also observed. In thin section were observed plagioclase and quartz (Fig. 3CO-a) and biotite in a glassy matrix. It is common to find red lava lithics surrounded by glass and plagioclase (Fig. 3CO-b). Were also observed vesiculate areas with crystals of plagioclase (Fig. 3CO-c).

Jamaica quarry is located 8 km to the south of Cuitzeo Lake, among Cuto del Porvenir, Cuparátaro and Téjaro villages (UTM *X*: 277920; *Y*: 2195993). Several deposits of ignimbrites compose the general stratigraphy of the region. The source or eruptive centre is not yet identified, but could be also associated to the SMC eruptive history. Particularly, Jamaica outcrop is composed by a grey-to-white ignimbrite lithofacies characterized by different proportions of

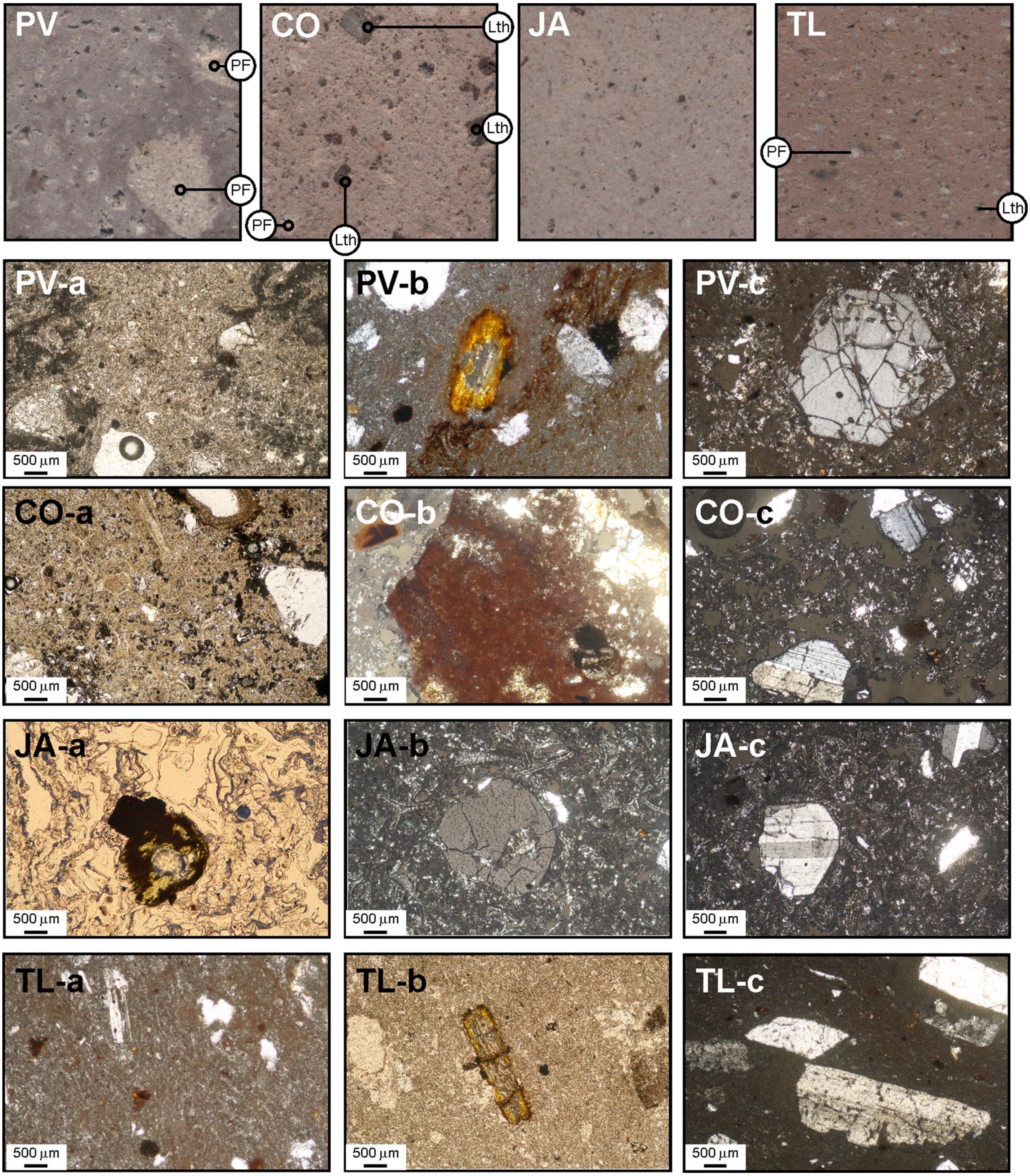


**Fig. 3** Images of the four studied rocks in hand sample: Piedra Vieja (PV); Cointzio (CO); Jamaica (JA); and Tlalpujahua (TL). Different pumice fragments (PF) and lithic fragments (Lth) are marked. Photomicrographies under petrographic microscope: quartz immersed in a glass matrix (**PV-a**), biotite with dark edges (**PV-b**), phenocrysts of quartz (**PV-c**), crystals of plagioclase in a glass matrix (**CO-a**), red lithic fragment (**CO-b**), plagioclases immersed in a glass matrix (**CO-c**), biotite associate with an oxide (**JA-a**), quartz in an eutaxitic matrix (**JA-b**), plagioclase in an eutaxitic glass matrix (**JA-c**), orthopyroxenes and plagioclase in a glass matrix (**TL-a**), clinopyroxene and oxides (**TL-b**) and plagioclase with trachytic texture (**TL-c**)

mm-to-cm size pumice (< 5 cm) and subrounded lithic lava clasts (< 2 cm) supported by a fine-rich matrix composed of glass, lithics and some phenocrysts. Bands or lents composed by accumulated fibrous pumices and phenocrysts are also observed. The phenocrysts consist of quartz, plagioclase and biotite in a welded matrix (Fig. 3JA-a to JA-c). The welded degree is observed in Fig. 3JA-a to JA-c where the matrix presents eutaxitic texture with shards of glass. Figure 3JA-a shows a biotite with dark rims, which is a common characteristic in all studied ignimbrites.

Tlalpujahua quarry is located within the Tlalpujahua township, in the oriental part of Michoacán state. Geologically, it corresponds to those described as Las Américas Formation (Corona-Chávez et al. 2000; De la Teja 2000; Morales-Gámez and Corona-Chávez 2006), regionally represented by different ignimbrites, distributed all along El Gigante, Majalco and Las Américas plateaus. Particularly, Majalco quarry is located 3 km to the north-west of Tlalpujahua city (UTM *X*: 375367; *Y*: 2192642). It is composed of two different layers of ignimbrites, basically lateral and vertically differentiated by the hydrothermal alteration degree and its associated physical characteristics. The not altered layer is greyish composed of very deformed black fragments forming fiammes, lithics of lavas and scarce proportion of pumice supported by a dense and vitric matrix. The hydrothermal altered layer is associated to the geometric and spatial distribution of the fractures. It is composed practically of the same components of not altered layer, on the contrary the black fragments highly contrast with the red and some times poorly made matrix. Thin sections contain phenocrysts of plagioclase, orthopyroxene immersed in a glassy matrix with eutaxitic texture (Fig. 3TL-a). In the photomicrographies TL-b and Tl-c (Fig. 3) can be observed crystals of clinopyroxene and plagioclase in a glassy matrix.

## Materials and methods

### Studied building stones

Four different rocks were studied: Piedra Vieja (PV), Jamaica (JA), Cointzio (CO) and Tlalpujahua (TL) ignimbrites (Fig. 3). The first one is the original building rock with which the main historical buildings of the old city of Morelia were built. The last three rocks are the construction materials used currently for restoration works.

Petrographic optical microscope (POM) was used in order to study the petrographic features of rocks. At least, two thin sections of each rock variety were examined under an Assioscop Zeiss transmitted light microscope. Mineral identification (qualitative analysis) of the rock clay fraction was carried out by means of XRD analysis on oriented aggregates.

All the studied samples correspond to welded rhyolitic ignimbrites with eutaxitic textures. In general terms, the observed minerals are quartz, plagioclase, orthopyroxene, oxides and biotites (Table 1). Lithics and pumice fragments are also observed. All these crystals and clasts are surrounded by a groundmass that, in general terms, constitutes around the 90% of the rock. Table 1 also shows the mineralogical identification of the clay fraction of the rocks.

### Durability tests

Two different durability tests were carried out: salt crystallization test and wet–dry test. Five samples of each kind of rock were tested in each one.

Salt crystallization test was carried out in accordance with the UNE-EN 12370 (1999) recommendations. Tested samples underwent cycles of saline immersion (14% w/w $Na_2SO_4$ solution, at 20 °C for 4 h), drying (at 60 °C for 16 h) and cooling at room conditions (20 °C, for 4 h). The rock resistance to salt weathering was quantified by means of the

**Table 1** Petrographic and mineralogical quantification of rock components

| | Mineral content [%] | | | | | Lth | PF | Gm | Clay mineralogy |
|---|---|---|---|---|---|---|---|---|---|
| | Qtz | Pl | Opx | Ox | Bt | [%] | [%] | [%] | |
| PV | 7.5 | 1 | – | 1 | 0.5 | – | * | 90 | Ka + Sm |
| JA | 1 | 8 | – | 0.5 | 1.5 | – | – | 89 | [Sm] |
| CO | – | 5 | – | 0.8 | 0.2 | 4 | 1 | 94 | Sm |
| TL | – | 10 | 2 | 1.5 | 0.5 | 0.5 | 1.5 | 87 | Mont |

Square brackets indicate trace contents

PV, Piedra Vieja; JA, Jamaica; CO, Cointzio; TL, Tlalpujahua; Qtz, quartz; Pl, plagioclase; Opx, orthopyroxene; Ox, oxides; Bt, biotite; Lth, lithics fragments; PF, pumice fragments; Gm, groundmass. Clay minerals: Ka, kaolinite; Sm, smectite; Mont, montmorillonite

*Pumice fragments in PV at this magnification are not observed. However, big pumice fragments (> 5 cm) are frequent in hand sample dry weight loss ($DWL_{salt}$), the alteration velocity (AV), the alteration index (AI) and the salt crystallization index (SC). AV is the final value of the derivative of the function representing the normalized weight as a function of the number of cycles (Angeli et al. 2006). AI is defined as the number of the cycle during which the first visible damage occurs (Angeli et al. 2006). SC is the alteration index based on visual observation proposed by Cardenes et al. (2014). This index is expressed in a 10 scale (10 for no altered samples and 0 for completely destroyed cubes).

The wet–dry test was conducted in parallel with the salt crystallization test. The steps, the timetable and the climatic conditions were the same. The only difference was that the saturation process of samples for 24 h in the vacuum vessel was carried out with distilled water (rather than $Na_2SO_4$ solution). A total number of 100 cycles was carried out. The dry weight loss after the test ($DWL_{wd}$) was calculated.

### Bulk density and porous system characterization

The bulk density, $\rho_{bulk}$, of a rock is defined as the ratio of its dry mass to its volume.

The open porosity to water ($\phi_{H_2O}$) was calculated using the vacuum water saturation test (after UNE-EN 1936). Open porosity to water is defined as the relationship between the volume of voids (ratio of absorbed water to water density) and the volume of the sample, expressed as a percentage.

Pore size distribution was quantified by means of mercury porosimetry. The open porosity to mercury ($\phi_{Hg}$) and mean pore size ($r_M$) were obtained by Autopore IV 9500 Micromeritics mercury porosimetry. The pore size interval ranges from 0.003 to 200 µm.

### Hydric properties

Ten prismatic blocks (20 × 20 × 60 mm) of each studied material were used for both the capillary and the atmospheric absorption tests as well as for the desorption test.

The capillary absorption test was carried out in accordance with UNE-EN 1925 (1999). Results were plotted as absorbed water per area of the sample against the square root of elapsed time. The capillary absorption coefficient, $C$, was calculated from the slope of the curve obtained.

Saturation coefficient ($S$) is the ratio of the volume of water absorbed (under atmospheric pressure) to total volume of connected voids in the rock (connected porosity).

For the evaporation test, samples are initially saturated with distilled water and they are placed in a desiccator with silica gel. Samples are weight at different time intervals in order to check the loss of water. Results were plotted as loss weight per area of the sample against the square root of elapsed time. This representation shows two parts: the first defines fast water evaporation and the second part defines slow water evaporation. Two different parameters were calculated from this curve. On the one hand, the evaporation coefficient, $E$, corresponds to the slope of the fast-evaporation part of the obtained curve. On the other hand, $W_e$ quantifies the amount (%) of water evaporated at the end of the test.

### Mechanical properties

Rock strength characterization was preformed using uniaxial compressive and ultrasonic tests. The uniaxial compressive test was carried out in accordance with the UNE-EN 1926 (2007).

The ultrasonic measurement was carried out with the same samples that were used in the water transport characterization tests. The transmission method was used, which consists of two piezoelectric sensors coupled to the sample at constant pressure.

Ultrasonic pulse velocity (UPV) was measured using $P$-wave polarized Panametric transducers (1 MHz) and a Sonic Viewer-170. A viscoelastic couplant (ultrasound eco-gel) was used to achieve good coupling between the transducer and the sample.

### Colour measurements

Due to the special importance of the aesthetic aspect of the materials employed in the restoration works of the Morelia's heritage, chromatic parameters of stone surfaces were determined in all the studied rock varieties. A spectrophotometer Minolta CM 2002 colorimeter was used. The results for D65 illuminant are presented in the CIE $- L^*a^*b^*C^*H$ parameters. The spectrophotometric mean values were taken from three measurements in both dry and wet rock conditions. The dry–wet chromatic variability allows to quantify not only the aesthetical aspect of rocks in normal (dry) conditions, but also during rainy periods or the appearance of stone pieces located in total/partial contact with water (fountains, rock skirting boards, etc.).

Perceptible visual changes are quantified by the total colour difference ($\Delta E^*$), which is defined as (Eq. 1):

$$\Delta E * = \left( (\Delta L *)^2 + (\Delta a *)^2 + (\Delta b *)^2 \right) \tag{1}$$

This parameter was calculated in order to quantify the visual change between the both wet and dry colour of the replacement rocks with respect to the original building rock (Piedra Vieja variety).

**Table 2** Petrophysic parameters measured in the studied rocks

| | PV | CO | JA | TL |
|---|---|---|---|---|
| Porous system characterization | | | | |
| $\rho_{bulk}$ [g/cm$^3$] | 1.85 ± 0.02 | 1.48 ± 0.03 | 1.68 ± 0.04 | 1.83 ± 0.03 |
| $\phi_{H_2O}$ [%] | 26.52 ± 0.80 | 40.36 ± 0.35 | 28.51 ± 2.11 | 26.79 ± 1.47 |
| $\phi_{Hg}$ [%] | 31.54 ± 5.32 | 42.95 ± 8.22 | 29.45 ± 5.50 | 28.05 ± 6.46 |
| $r_M$ [μm] | 2.22 | 3.05 | 5.22 | 2.16 |
| Pore size distribution [%] | | | | |
| [< 0.01 μm] | 0.00 | 0.05 | 2.62 | 2.47 |
| [0.01–0.1 μm] | 13.27 | 4.27 | 4.58 | 6.00 |
| [0.1–1 μm] | 35.87 | 30.07 | 18.37 | 41.65 |
| [1–10 μm] | 42.87 | 60.80 | 68.69 | 44.10 |
| [10–100 μm] | 2.60 | 1.49 | 3.34 | 3.88 |
| [> 100] | 5.37 | 3.30 | 2.42 | 1.88 |
| Microporosites [%] | | | | |
| $P_{m1}$ | 15.01 | 14.77 | 5.49 | 13.56 |
| $P_{m2.5}$ | 25.66 | 35.60 | 10.96 | 24.73 |
| $P_{m5}$ | 27.39 | 39.93 | 18.79 | 25.21 |
| Hydric properties | | | | |
| $S$ [–] | 0.75 ± 0.03 | 0.88 ± 0.03 | 0.55 ± 0.01 | 0.66 ± 0.05 |
| $C$ [kg/(m$^2$h$^{0.5}$)] | 0.24 ± 0.01 | 0.76 ± 0.02 | 0.05 ± 0.01 | 0.20 ± 0.01 |
| $E$ [kg/(m$^2$h$^{0.5}$)] | − 0.12 ± 0.01 | − 0.12 ± 0.02 | − 0.05 ± 0.01 | − 0.08 ± 0.01 |
| $W_e$ [%] | 95.61 ± 2.1 | 97.36 ± 3.6 | 64.61 ± 5.2 | 94.71 ± 2.4 |
| Mechanical properties | | | | |
| $\sigma_c$ [MPa] | 30.77 ± 8.74 | 7.23 ± 0.58 | 32.38 ± 15.09 | 45.78 ± 9.08 |
| UPV [km/s] | 3.13 ± 0.32 | 1.91 ± 0.52 | 3.25 ± 0.49 | 2.69 ± 0.46 |
| Durability | | | | |
| $DWL_{salt}$ [%] | 6.53 ± 1.46 | 72.36 ± 12.27 | 23.74 ± 27.53 | 10.06 ± 5.43 |
| $DWL_{wd}$ [%] | 0.01 ± 0.00 | 0.05 ± 0.02 | 0.01 ± 0.00 | 0.01 ± 0.00 |
| AI | 20 | 4 | 21 | 18 |
| AV | 0.22 | 2.89 | 0.79 | 0.34 |
| SC | 9.68 | 4.58 | 7.92 | 9.58 |

PV, Piedra Vieja; CO, Cointzio; JA, Jamaica; TL, Tlalpujahua; $\rho_{bulk}$, bulk density; $\phi_O$, open porosity; $\phi_{Hg}$, connected porosity; $r_M$, mean pore size; $C$, capillary absorption coefficient; $S$, saturation coefficient; $E$, evaporation coefficient; $W_e$, water evaporated during desorption test; $\sigma_c$, rock strength; UPV, ultrasonic pulse velocity ($P$-waves); $DWL_{salt}$, dry weight loss during salt crystallization test; $DWL_{wd}$, dry weight loss during wet–dry test; AI, the alteration index; AV, the alteration velocity; SC, the salt crystallization index

## Results and discussion

### Durability and decay patterns of studied building stones

Table 2 shows the obtained values of the petrophysical characterization of the studied rocks. CO variety results the most porous rock ($\phi_{H_2O}$ ~ 40%) and its porous system is well connected, offering a rapid and direct water transfer from the inner to the outside part of the rock, and vice versa (CO shows the highest values of $S$, $C$, $E$ and $W_e$ values, Table 2). On the contrary, despite the fact that the JA variety is not the less porous rock ($\phi_{H_2O}$ ~ 28.5%), its porous system is the worst connected (the lowest values of $S$, $C$, $E$ and $W_e$ are measured in JA, Table 2). Water movement through this rock is difficult and needs a lot of time for going out or going into the block.

From the durability point of view, Morelia's ignimbrites show very low weight losses during wetting–drying processes ($DWL_{wd}$ in Table 2) despite of both the presence of expansive clays (smectite and montmorillonite, Table 1) and the high number of wet–dry cycles carried out (100 cycles in total). Similar ignimbrites used in the architectural heritage of other Mexican colonial cities show an intense weathering after this test (i.e. Loseros Tuff of Guanajuato) (López-Doncel et al. 2013). The low effectiveness of the differential swelling in the studied rocks is due to their welded structure and high strength (Madsen and Müller-Vonmoos 1989; Ostroumov 2009).

On the contrary, studied ignimbrites are highly sensitive to salt crystallization processes. In general terms, durability of ignimbrite-type rocks against salt crystallization is conditioned by their welding degree (related to porosity and mechanical resistance), preferential orientations of components and mineralogical content (Özvan et al. 2015). On the one hand, CO is the softest variety mainly due to its high porosity, its pore size distribution (one main pore population centred between 0.1 and 1 µm) and low mechanical resistance. On the other hand, PV results the most durable rock variety. According to the AI and AV classifications proposed by Angeli et al. (2007), CO presents low AI and medium AV indicating that is characterized by early visible damage and a progressive and fast disintegration during the salt crystallization test up to be almost completely broken down. The other three varieties have low alteration velocities (AV < 1%) and medium alteration index for TL (AI between 10 and 18) and high for both PV and JA (AI > 19). It means that JA and, especially, PV remain practically unweathered over the whole ageing test, being able to observe slight visual deterioration at the end of the test.

Figure 4 shows the weight loss evolution of each studied rock during the salt crystallization test. The three stages proposed by Angeli et al. (2007) are included in Fig. 4. These stages describe the weight evolution of samples as a competition between the loss of material and the salt filling of pores. They are: (1) weight increase due to salt supply; (2) weight variation depending on a equilibrium between salt supply and stone damage; and (3) weight decrease because salt uptake becomes negligible compared to stone damage. Rock samples studied in this paper show two different decay modes during phase III. On the one hand, the linear decay mode occurs when the weight loss after the first visual damages increases progressively as the cycles draw on. It occurs in CO and PV. On the other hand, the nonlinear decay mode is characterized by sudden slope changes in the weight loss curve. For instance, TL and JA samples remain practically unweathered (or slightly decayed) during the most part of the test, but at a certain threshold, rapid weight losses are registered in a small number of cycles. The threshold-based episodic decay pathway has been extensively described in the context of stone decay by Smith et al. (2008, 2010). The seemingly unpredictable, episodic and sometimes catastrophic breakdown is particularly common in sandstones (Smith et al. 2008) but also found in limestones (Smith et al. 2010; Martínez-Martínez et al. 2013). On the contrary, decay behaviour in ignimbrite-type rocks has been always described according to a linear system (Topal and Sözmen 2003; Yavuz 2012; Korkanç 2013; Özbek 2014). Results obtained in this study show that in some cases, especially in strong welded ignimbrites, nonlinear weathering evolution can be developed. A deep discussion about these two different decay modes is carried out in the sequent subsection.

Three different decay forms are developed during the salt crystallization test (Fig. 4). Most of PV and TL samples show differential erosion with loss of weak components (pumice fragments in PV and small both lithic fragments

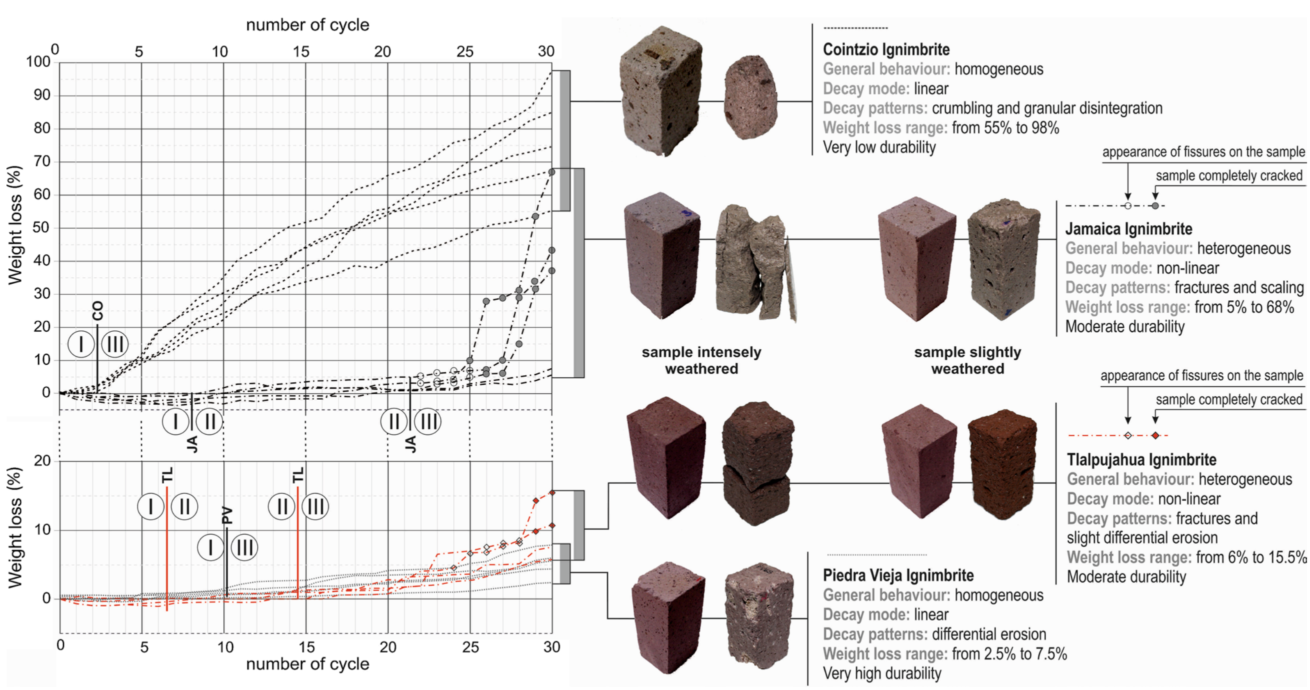


**Fig. 4** Weight loss evolution during the salt crystallization test, showing some examples of different weathered samples (before and after the test)

and pumices in TL). TL shows fiammes structures preferentially oriented and fractures can develop related to these weak planes. JA variety suffers scaling whilst CO samples are intensely decayed by means of granular disintegration, showing rounded borders and softening shapes. The development of each kind of decay form (scaling or granular disintegration) is controlled by the hydric properties. If liquid water transfer towards the surface is possible during most of the drying phase, alteration will occur very close to the stone's surface (Vergès-Belmin 2010). Consequently, granular disintegration tends to develop in rocks with high both $E$ and $W_e$ values (CO in Table 2). On the contrary, the formation of subefflorescences and scaling is more important in rocks with low evaporation coefficients and poorly connected porous systems (JA variety).

Finally, in order to evaluate the regularity of the weathering of a set of samples from the same type of stone, Angeli et al. (2007) differentiate two kinds of global behaviours: homogeneous and heterogeneous. Homogeneous general behaviour refers to those stones that present a constant decay pattern, and it is regular for one sample and approximately the same from a sample to another. For example, CO and PV (Fig. 4) give good examples of this alteration. On the other hand, JA and TL present various alteration behaviours from one sample to another. This is due to pre-existent heterogeneities in the rock, such as big pumices or preferential oriented structures (fiammes in TL). These heterogeneities act as local weakness, and thus differential weathering can occur.

## Porosimetric control of salt crystallization damages

Breakage of stone is due to physical action of salts crystallizing into its pore network when crystallization pressure exceeds the tensile strength of the stone. The pressure reached during the process depends on the pore size distribution and it is quantified by means of Eq. 2 (Wellman and Wilson 1965):

$$\Delta P = 2\sigma\left(\frac{1}{r} - \frac{1}{R}\right) \tag{2}$$

where $\sigma$ is the salt solution interfacial tension, $r$ and $R$ are the radii of the small and coarse pores, respectively. To calculate the effective pressure which can arise specifically in the studied stones, it is necessary to consider the volume percentage of the pores of each class ($V_r$), which should be related to the volume percentage of coarse pores ($V_R$). Multiplying the factor $V_r/V_R$ for the theoretical pressure of each class permits calculation of the effective pressure value $P_{eff}$. The sum of the effective pressure of each class will give the total pressure (tension) that the material will support when the salt crystallizes.

Table 3 shows the effective pressures obtained for the studied rocks, considering some of the most frequent salts observed in the building stones of the architectural heritage (Vergès-Belmin 2010): halite, thenardite, mirabilite and epsomite. Pores are grouped according to radii (expressed in μm) into five classes in the following ranges: class I, $r < 0.01$; class II, $r = 0.01$–$0.1$; class III, $r = 0.1$–$1$; class IV, $r = 1$–$10$; and class V, $r = 10$–$100$. The median radii ($r$) of pore classes I–IV are: 0.005, 0.05, 0.5 and 5, respectively.

**Table 3** Pore size distribution and effective pressures reached during the salt crystallization process inside the pore system of studied rocks

| | Pore volume [%] | | | | | | Effective pressure [MPa] | | | | $P_T$ |
|---|---|---|---|---|---|---|---|---|---|---|---|
| | Class I | Class II | Class III | Class IV | Class V | | Class I | Class II | Class III | Class IV | [MPa] |
| CO | 0.00 | 13.27 | 35.87 | 42.87 | 2.60 | H | 1.18 | 9.53 | 6.72 | 1.36 | 18.80 |
| | | | | | | TH | 0.57 | 4.57 | 3.22 | 0.65 | 9.01 |
| | | | | | | M | 0.65 | 5.25 | 3.70 | 0.75 | 10.36 |
| | | | | | | EPS | 0.74 | 5.94 | 4.18 | 0.85 | 11.71 |
| JA | 0.05 | 4.27 | 30.07 | 60.80 | 1.49 | H | 26.23 | 4.58 | 1.84 | 0.69 | 33.33 |
| | | | | | | TH | 12.56 | 2.19 | 0.88 | 0.33 | 15.97 |
| | | | | | | M | 14.45 | 2.52 | 1.01 | 0.38 | 18.36 |
| | | | | | | EPS | 16.33 | 2.85 | 1.14 | 0.43 | 20.76 |
| TL | 2.62 | 4.58 | 18.37 | 68.69 | 3.34 | H | 21.27 | 5.17 | 3.58 | 0.38 | 30.40 |
| | | | | | | TH | 10.19 | 2.48 | 1.72 | 0.18 | 14.56 |
| | | | | | | M | 11.72 | 2.85 | 1.97 | 0.21 | 16.75 |
| | | | | | | EPS | 13.25 | 3.22 | 2.23 | 0.24 | 18.93 |
| PV | 2.47 | 6.00 | 541.65 | 44.10 | 3.88 | H | 0.03 | 17.06 | 4.61 | 0.55 | 22.26 |
| | | | | | | TH | 0.02 | 8.17 | 2.21 | 0.26 | 10.66 |
| | | | | | | M | 0.02 | 9.40 | 2.54 | 0.30 | 12.26 |
| | | | | | | EPS | 0.02 | 10.62 | 2.87 | 0.34 | 13.86 |

H, halite; Th, thenardite; M, mirabilite; EPS, epsomite; $P_T$, total pressure

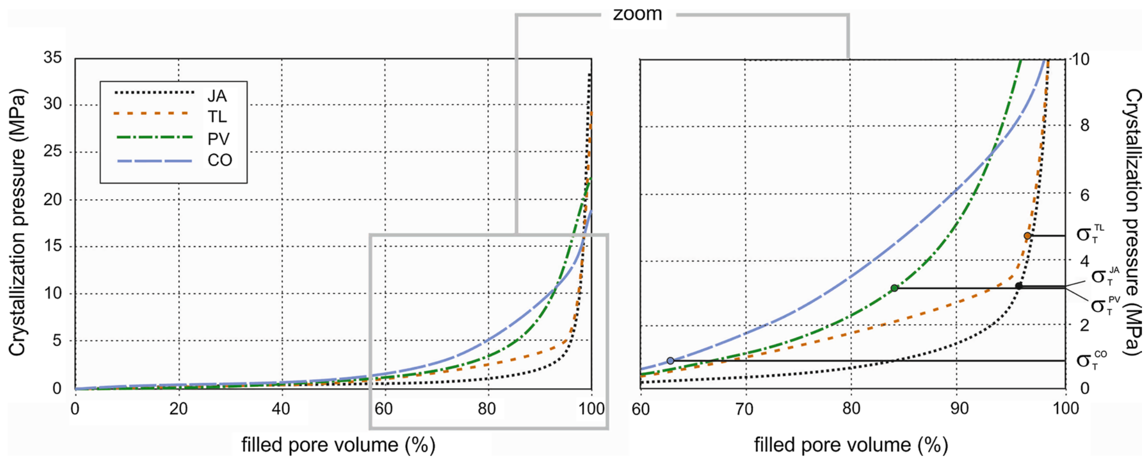


**Fig. 5** Estimation of crystallization pressures of halite in the porous system of the studied rocks. Values of tensile strength ($\sigma_T$) for all samples are shown

Class V ($R = 50$ µm) is considered the one where preferential crystal growth takes place.

The values of salt solution interfacial tension ($\sigma$) of each salt are (La Iglesia et al. 1997; Rodriguez-Navarro and Dohene 1999): 0.083 N/m for halite; 0.04 N/m for thenardite; 0.046 N/m for mirabilite; and 0.052 N/m for epsomite. According to these values, and in agreement with the values of total pressure ($P_T$) shown in Table 3, the order of the disruptive effect of the salts considered in this study is as follows: halite > epsomite > mirabilite > thenardite. This ranking has been established theoretically after the values obtained in Eq. 2. Consequently, the real damage provided by these salts must be confirmed experimentally in the future.

La Iglesia et al. (1997) assert that salt crystallization in porous media takes place in the first moment in the largest pores and continues in the smaller pores. After their methodology, we can calculate the effective pressure reached in the porous system of the rock at different percentages of pores filled with salt during the salt crystallization process. Figure 5 shows the variation of pressure against the percentage of pores filled in the studied materials (halite is taken as an example). Crystallization pressures in CO and PV increases rapidly and it takes high values during the salt supply. On the contrary, JA only reaches significant crystallization pressures when most of the room where salt can crystallize has been filled up. However, the total crystallization pressure reached when all the porous system is occupied is higher in JA (33.3 MPa for halite, Table 3) than in CO and PV (18.8 and 22.3 MPa for halite, respectively).

Salt damages occur when the salt crystallization pressure is greater than the cohesive forces of the material. The uniaxial tensile strength reflects at a macroscopic scale these cohesive forces. When the crystallization pressure exceeds the tensile strength, the material cracks. Tensile strengths have been deduced from the measured values of simple compression in dry conditions (Table 2), following Griffith's theory (Griffith 1924). This theory postulates that the strength of brittle materials like rock in compression should be approximately 10 times the tensile strength. With this in mind, the tensile strengths of the studied rocks are as follows: 3.1 MPa for PV; 0.7 MPa for CO; 3.2 MPa for JA; and 4.6 MPa for TL. These values are shown in Fig. 5. In the case of CO, the tensile strength limit is reached with low contents of any salt (~ 60%). However, in the case of JA and TL samples only after approximately 95% filling of the pores, the crystallization pressure approaches the tensile strength limit.

These differences explain the two decay models showed during the salt crystallization test (linear and nonlinear decay modes). Effective pressure in CO increases rapidly and salt crystallization pressure can generate damages when the porous system is only partially filled with salts. Consequently, the weathering response is fast and visual damages are observed during the salt uptake even when there is still room in the sample for salt to crystallize. In the cases of JA and TL, damages are visible only when almost all the pores are filled. Consequently, crystallization stresses only are great enough when high salt quantities crystallize inside the porous system. This fact contributes to explain the nonlinear decay mode observed in JA during the salt crystallization test.

## Validity of durability estimators

Determining the stone susceptibility to salt crystallization pressure using structural and mechanical parameters is well reported in the literature. Table 4 shows some of the proposed durability estimators based on different rock properties (a deeper revision of these parameters can be found

**Table 4** Rock durability estimators published in bibliography

| Durability estimator | Parameters used in durability estimation | References |
|---|---|---|
| Durability factor: $D = C_s \cdot P$ | $C_s$ = saturation coefficient (parameter $S$ in this work)<br>$P$ = total porosity | Richardson (1991) |
| Durability estimator: $D = \left[\left(P \cdot P_{\text{micro}}\right)^{C_s}\right]^{0.5}$ | $P$ = total porosity<br>$P_{\text{micro}}$ = microporosity (volume of pores with radius smaller than 2.5 µm) (parameter $P_{m2.5}$ in this work)<br>$C_s$ = saturation coefficient (parameter $S$ in this work) | Mod'd et al. (1996) |
| Durability dimension estimator: $\text{DDE} = \sum \frac{\vartheta(r)}{r} \cdot P_c$ | $\vartheta(r)$ = porosity fraction with pore radius $r$<br>$r$ = pore radius<br>$P_c$ = connected porosity (parameter $\phi_{\text{Hg}}$ in this work) | Ordóñez et al. (1997) |
| Petrophysical durability estimator: $\text{PDE} = \frac{\text{DDE}}{\sigma_c}$ | DDE = durability dimension estimator (Ordóñez et al. 1997)<br>$\sigma_c$ = rock strength | Benavente et al. (2004) |
| Alteration index estimator: $\text{AI}_{\text{estim}} = \ln\left(\frac{100C}{E \cdot \sqrt{\sigma_t}}\right)$ | $C$ = capillary coefficient<br>$E$ = evaporation coefficient<br>$\sigma_t$ = tensile strength | Angeli et al. (2007) |
| Salt susceptibility index: $\text{SSI} = \left(I_{P_c} + I_{P_{m0.1}}\right) \cdot \left(\frac{P_{m5}}{P_c}\right)$ | $I_{P_c}$ = index of total connected porosity<br>$I_{P_{m0.1}}$ = index of microporosity of pores smaller than 0.1 µm in radius<br>$P_{m5}$ = microporosity of pores smaller than 5 µm in radius<br>$P_c$ = total connected porosity (parameter $\phi_{\text{Hg}}$ in this work) | Yu and Oguchi (2010) |

**Table 5** Bivariate Pearson's correlation coefficients between the parameters for quantifying the rock salt weathering and different published durability estimators

| | [1]$\text{AI}_{\text{estim}}$ | [2]SSI | [3]D | [4]D | [5]DDE | [6]PDE | C | UPV | $\sigma_c$ |
|---|---|---|---|---|---|---|---|---|---|
| $\text{DWL}_{\text{salt}}$ | 0.73 | *0.43* | 0.70 | 0.60 | 0.64 | **0.95** | 0.76 | 0.71 | 0.82 |
| AI | **0.97** | 0.75 | 0.88 | 0.79 | *0.49* | **0.97** | **0.96** | **0.94** | **0.85** |
| AV | 0.77 | *0.48* | 0.74 | 0.65 | 0.64 | **0.97** | 0.80 | 0.74 | 0.83 |
| SC | 0.64 | *0.49* | 0.73 | 0.68 | 0.66 | **0.90** | 0.75 | 0.74 | 0.82 |

Measured parameters: rock resistance to salt weathering ($\text{DWL}_{\text{salt}}$); alteration index (AI); alteration velocity (AV); salt crystallization index (SC); capillary absorption coefficient ($C$); ultrasonic pulse velocity (UPV); and rock strength ($\sigma_c$). Published durability estimators: [1]Alteration index estimator (Angeli et al. 2007); [2]Salt susceptibility index (Yu and Oguchi 2010); [3]Durability factor (Richardson 1991); [4]Durability estimator (Mod'd et al. 1996); [5]Durability dimension estimator (Ordóñez et al. 1997); and [6]Petrophysical durability estimator (Benavente et al. 2004). In bold font: very good correlation ($R^2 > 0.9$). In italics: poor correlation ($R^2 < 0.5$)

in Benavente et al. 2004 and Yu and Oguchi 2010). Most of them are based on pore characteristics as porosity, open porosity and pore size distribution. Other petrophysical properties used frequently in these equations are those quantifying the hydric behaviour of the rock (i.e. water absorption coefficient, saturation coefficient or evaporation coefficient). Moreover, because salt crystallization produces stress over pore surfaces, it is reasonable to assume that stone resistance to weathering is related also to stone strength (Benavente et al. 2004).

UNE-EN 12370 (1999) recommends that rock durability should be quantified by means of the dry weight loss during the ageing test. This parameter (DWL) is widely used due to easiness and objectivity. However, other authors suggest that rock weathering cannot be always measured by means of the material loss (i.e. a partial cracking) (Angeli et al. 2007; Cardenes et al. 2014). They propose alternative parameters, based on visual observation, for quantifying the damages as well as the decay velocity (Ai, Av and SC). Table 4 shows the values obtained for the studied rocks.

Table 5 shows the obtained Pearson's correlation index between the durability estimators published in bibliography and the different parameters proposed for quantifying the rock decay achieved during the artificial ageing tests. The statistical analysis was carried out with the program SPSS v.15.0 for Window, assuming that the relationships between the variables are linear.

Results reveal that the behaviour predicted by the theoretical estimators best fits the visual weathering suffered by the rocks than its mass loss. In fact, most of the lowest Pearson's correlation indexes for each estimator are obtained with the $\text{DWL}_{\text{salt}}$ parameter. This result highlights the fact that in many cases, the weathering degree suffered by a rock cannot be completely described only by means of the dry weight lost as standards suggest (UNE-EN 12370), but other additional parameters are needed (Angeli et al. 2007).

The capillary absorption coefficient (*C*) is closely related to pore structure by the effective radius and the porosity (Leventis et al. 2000). Thus, rocks with narrow pores produce a low capillary absorption coefficient value (Leventis et al. 2000; Benavente et al. 2004). This coefficient is sometimes considered as a durability estimator due to the strong influence of pore structure on both the capillary absorption coefficient and the salt crystallization resistance (Richardson 1991; Benavente et al. 2004; Angeli et al. 2006). Results from this study confirm the good approximation that the capillary absorption coefficient performs the rock durability, quantified by means of the high Pearson's correlation coefficients obtained for *C* and *D* (Durability factor, Richardson 1991).

Benavente et al. (2004) assert that the strength of the stone is an essential parameter in determining its durability because of the fact that it is the material resistance to crystallization pressure. Consequently, this mechanical parameter can improve substantially those durability estimators based exclusively on the rock pore structure. These assertions agree the obtained results in this paper. The best correlations are obtained for those estimators in which the mechanical properties of the rock are taken into account ($AI_{estim}$ and, especially, PDE).

Finally, *C*, UPV and $\sigma_c$ are revealed as useful direct petrophysical parameters that can act as simple durability estimators. Although these parameters do not show the highest correlation coefficients (Table 5), the obtained correlations are much better than the coefficients for other complex estimators obtained in this study (SSI and DDE, for example). UPV is especially interesting due to its non-destructive nature. The existence of pores, microcracks and joints between grains inside the rock, as well as their apparition during weathering processes, reduce the *P*-waves velocity (Martínez-Martínez et al. 2011). Consequently, the UPV can estimate the weathering degree of a rock as well as its long-term behaviour.

## Recommendations for selecting future stone replacement

When a new rock is selected for using it in the restoration process of a monument, it must guarantee a good durability as well as a good compatibility with the pre-existing building materials. Moreover, in the specific case of the city of Morelia, specific aesthetical requirements are imposed to the new used rock in order to preserve the visual homogeneity of the historical constructions.

From an aesthetical point of view, CO ignimbrite offers the highest chromatic compatibility with the original building rock, followed by JA which also presents similar chromatic parameters with PV. This assertion is based on chromatic data shown in Table 6, taking into account that perceptible visual changes are achieved only when the total colour difference parameter exceeds three CIELAB units ($\Delta E^* > 3$) (Urosevic et al. 2013). According to this criteria, TL is the rock with the highest chromatic difference ($\Delta E^*$ = 17.41 and 20.46 in wet and dry conditions,

**Table 6** Mean values and standard deviation of chromatic parameters and their variations in studied rocks

| Sample | PV | | CO | | JA | | TL | |
|---|---|---|---|---|---|---|---|---|
| | Wet | Dry | Wet | Dry | Wet | Dry | Wet | Dry |
| *L** | | | | | | | | |
| Mean | 31.24 | 50.76 | 28.78 | 45.78 | 25.52 | 46.22 | 13.98 | 30.30 |
| $\sigma$ | 3.87 | 2.34 | 1.56 | 6.04 | 0.23 | 1.11 | 0.47 | 1.71 |
| *a** | | | | | | | | |
| Mean | 1.72 | 1.26 | 3.93 | 3.45 | 0.75 | 0.41 | 2.97 | 3.08 |
| $\sigma$ | 0.29 | 0.16 | 0.11 | 0.49 | 0.10 | 0.46 | 0.24 | 0.13 |
| *b** | | | | | | | | |
| Mean | 5.69 | 7.62 | 7.33 | 9.66 | 4.96 | 7.85 | 3.86 | 6.25 |
| $\sigma$ | 1.38 | 0.98 | 0.56 | 0.35 | 0.36 | 0.53 | 0.12 | 0.13 |
| *C** | | | | | | | | |
| Mean | 5.95 | 7.73 | 8.32 | 10.27 | 5.01 | 7.87 | 4.87 | 6.96 |
| $\sigma$ | 1.40 | 0.98 | 0.48 | 0.18 | 0.37 | 0.55 | 0.25 | 0.06 |
| *H** | | | | | | | | |
| Mean | 72.99 | 80.57 | 61.71 | 70.30 | 81.36 | 87.09 | 52.46 | 63.75 |
| $\sigma$ | 1.13 | 0.96 | 2.19 | 3.23 | 0.46 | 3.12 | 1.39 | 1.42 |
| Visual colour change between both replacement and original rocks | | | | | | | | |
| $\Delta E^*$ | | | 3.68 | 5.81 | 5.85 | 4.63 | 17.41 | 20.59 |

PV, Piedra Vieja ignimbrite; CO, Cointzio ignimbrite; JA, Jamaica ignimbrite; TL, Tlalpujahua ignimbrite. Chromatic parameters: *L** brightness; *a** red-green components; *b** yellow-blue components; *C** chroma; *H** Hue respectively), being especially darker, redder and bluer than the reference stone.

In general terms, significant colour differences between wet and dry surfaces were measured in the whole studied rocks (Table 6). The general trend in all the cases became brighter, more yellow and more blue in dry conditions (quantified by higher values of $L^*$ and $b^*$ and lower values of $a^*$, respectively), with the only exception of TL, whose dry surface became more red (higher $a^*$ in dry conditions). These values reveal that the valued pinkish aspect of the building rocks is more noticeable when they are dry (more common situation), except for TL variety that is pinker when it is wet.

However, contrarily to these results, TL is highlighted as the most suitable rock when petrophysic criteria are applied. This assertion is supported on both its durability and the high compatibility with PV, as it is discussed below.

According to its durability during the salt crystallization test, TL is the most resistant rock among the three proposed replacement stones. The only preventive measure for using TL variety is placing rock blocks with the preferential planes (marked by its pumices and lithic fragments) in horizontal position, in order to avoid flaking and scaling.

In restorations to be carried out on historical buildings, it is also highly important to select stones that exhibit similar porosity and hydric behaviours to that of the original stone (Graue et al. 2011; Korkanç 2013). Deterioration can develop faster in buildings where stones of varying physical properties are used in adjacency, particularly on the stones that have weaker properties due to their high porosity and water absorption levels. In fact, the high porosity of some ignimbrites and transport of water mediated by capillarity accelerate their deterioration state (Özvan et al. 2015). Furthermore, the wet surfaces of stone are the appropriate substrate for the biological patina development. Due to all these reasons, TL is confirmed as the most suitable building stone among the studied varieties. Samples of both TL and PV show the same behaviour during capillary uptakes and water absorption and desorption (Table 2). That fact guarantees the correct coexistence of rock blocks placed together in the building.

On the contrary, the variety of CO is revealed as the worst restoration stone. On the one hand, its durability is extraordinarily low (some severe decay patterns were observed after only five cycles of salt crystallization test). This low resistance is also demonstrated by the high degradation degree observed in the monuments restored during the last decades in which this rock was used (Fig. 1). On the other hand, the facility with which water can access as well as go out from the rock is an inconvenient property. This accessibility allows salty water to fill the porous system and the later evaporation causing the salt crystallization.

JA variety shows an intermediate salt weathering resistance between TL and CO, and moreover, its aesthetical properties are very similar to those of the original building rock. Therefore, JA could be another admissible building stone for replacing the original blocks of PV in the monuments of Morelia. However, according to its hydric properties, the water flux through this rock is more difficult than in the original building rock (PV). Consequently, it uses in restoration works cause predictably the acceleration and worsening of the weathering state of the original rock blocks of PV.

## Conclusions

Piedra Vieja (PV) is a rhyolitic ignimbrite used as original building rock in the architectural heritage of Morelia city (Michoacán state, México). Its historical quarries are nowadays under the new urban expansion areas. Consequently, three different ignimbrites have been used during the last decades as replacement materials: Cointzio (CO), Jamaica (JA) and Tlalpujahua (TL) stones. In this paper, a deep analysis of the weathering process of all these rocks during wet–dry and salt crystallization cycles is carried out. The following conclusions may be drawn from the obtained results:

- Studied ignimbrites present moderate-high porosity values ranging from 26% (PV and TL varieties) to more than 40% (CO). Despite the fact that the JA variety is not the less porous rock (28%), its porous system is the worst connected, showing the lowest coefficients in the capillary absorption test and the desorption test (0.05 and $-$ 0.05 kg $m^{-2}$ $h^{-0.5}$, respectively). On the contrary, CO variety results the most porous rock and its porous system is well connected, offering high coefficients ($C = 0.76$ kg $m^{-2}$ $h^{-0.5}$ and $E = -$ 0.12 kg $m^{-2}$ $h^{-0.5}$). All these properties are directly related to the durability of rocks and also to the decay patterns developed on them. CO shows granular disintegration due mainly to its high both $E$ (evaporation coefficient) and $W_e$ (water evaporated during desorption test) values. On the contrary, the subefflorescences and scales observed in JA are directly related to its low evaporation coefficients and poorly connected porous systems. The low mechanical resistance of CO also favours its low durability (weight loss higher than 70%). PV and TL result the most resistant rocks during salt crystallization test due to both their low porosity and welded structures.
- Two different decay modes are recognized during the salt crystallization test depending on the progressive (linear) or sudden (nonlinear) weight loss as the cycles draw on. These two decay modes are explained after the effective pressure reached in the porous system at different percentages of pores filled with salt during the salt crys-

tallization process. Effective pressure in CO increases rapidly and salt crystallization stress can generate damages when the porous system is only partially filled with salts (~ 60%). Consequently, the weathering response is fast and visual damages are observed during the salt uptake even when there is still room in the sample for salt to crystallize (linear decay mode). In the cases of JA and TL, damages are visible only when almost all the pores are filled (> 95%). Consequently, crystallization stresses only are great enough when high salt quantities crystallize inside the porous system, remaining quasi-unweathered during the filling process.

- The presence of expansive clays (smectite and montmorillonite) suggests the possibility of weathering by wet–dry cycles, as it is proved for similar rocks in bibliography. However, the low clay content and the welded structure of the Morelia's ignimbrites counteract the swelling effects. Results show very low weight losses at the end of the test (< 0.1% in all the samples).
- Petrophysical durability estimator (PDE), proposed by Benavente et al. (2004), results the most accurate theoretical estimator for assessing the dry weight loss of Morelia's ignimbrites during the salt crystallization test. The main goal of this parameter is to take into account not only the pore size distribution but also the mechanical properties of the rock. On the other hand, UPV (ultrasonic pulse velocity) is revealed as a useful, direct and non-destructive parameter that can act as simple durability estimator. However, obtained results conclude that, in general terms, numerical estimators quantify better the visual weathering suffered by the studied rocks than its mass loss.
- According to the aesthetical criteria and to the spectrophotometry measurements, CO results the most suitable rock variety after the chromatic similarity with the original building stone (PV). Nevertheless, the petrophysical analysis contradicts the visual selection: TL is the most advisable rock for restoration purposes after its good both durability and compatibility with PV, whilst CO is the worst option. This result highlights the importance of carrying out the selection of building stones for restoration works according to petrophysical criteria, instead of using exclusively an aesthetic valuation. The selection of a replacement stone compatible petrophysically with the original building rock contributes to guarantee more effective restoration works and to preserve correctly the architectural heritage of cities.

## References


Alonso E, Martínez L (2003) The role of environmental sulfur on degradation of ignimbrites of the Cathedral in Morelia, Mexico. Build Environ 38:861–867

Andriani G, Walsh N (2003) Fabric, porosity and water permeability of calcarenites from Apulia (SE Italy) used as building and ornamental stone. Bull Eng Geol Environ 62(1):77–84

Angeli M, Bigas JP, Menéndez B, Hébert R, David C (2006) Influence of capillary properties and evaporation on salt weathering of sedimentary rocks. In: Fort R, Alvarez de Buergo M, Gomez-Heras M, Vezquez-Calvo C (eds) Heritage, weathering and conservation. Taylor & Francis/Balkema, Leiden, pp 253–259

Angeli M, Bigas JP, Benavente D, Menéndez B, Hébert R, David C (2007) Salt crystallization in pores: quantification and estimation of damage. Environ Geol 52:205–213

Benavente D, García-del-Cura MA, Fort R, Ordóñez S (2004) Durability estimation of porous building stones from pore structure and strength. Eng Geol 74:113–127

Cardenes V, Mateos FJ, Fernández-Lorenzo S (2014) Analysis of the correlations between freeze–thaw and salt crystallization tests. Environ Earth Sci 71:1123–1134

Chen TC, Yeung MR, Mori N (2004) Effect of water saturation on deterioration of welded tuff due to freeze–thaw action. Cold Reg Sci Technol 38:127–136

Cisneros-Máximo G (2015) Estudio geológico-geomorfológico de los volcanes Tetillas-Quinceo. Propuesta de cartografía Jerárquica. Maestría en geografía. Facultad de Filosofía y Letras; Universidad Nacional autónoma de México, Morelia, Michoacán

Columbu S, Gioncada A, Lezzerini M, Marchi M (2014) Hydric dilatation of ignimbritic stones used in the church of Santa Maria di Otti (Oschiri, northern Sardinia, Italy). Ital J Geosci 133(1):149–160

Corona-Chávez P, Mennella L, Salgado-Soto Z, Garduño-Monroy VH (2000) Carta geológico-minera de la hoja Angangueo, escala 1: 50000, con notas explicativas. Consejo de Recursos Minerales-Secofi, México

De la Teja G (2000) Carta geológico-minera de la hoja El Oro, escala 1: 50000, con notas explicativas. Consejo de Recursos Minerales-Secofi, México

Di Benedetto C, Cappelletti P, Favaro M, Graziano SF, Langella A, Calcaterra D, Colella A (2015) Porosity as key factor in the durability of two historical building stones: neapolitan Yellow Tuff and Vicenza Stone. Eng Geol 193:310–319

Ferrari L, Garduño VH, Pasquaré G, Tibaldi A (1994) Volcanic and tectonic evolution of central México: oligocene to present. Geofis Int 33(1):91–105

Garduño-Monroy VH, Arreygue-Rocha E, Israde-Alcántara I, Rodríguez-Torres G (2001) Efectos de las fallas asociadas a sobreexplotación de acuíferos y la presencia de fallas potencialmente sísmicas en Morelia, Michoacán, México. Revista Mexicana de Ciencias Geológicas 18(1):37–54

Gómez-Vasconcelos MG, Garduño-Monroy VH, Macías JL, Layer PW, Benowitz JA (2015) The Sierra de Mil Cumbres, Michoacán, México: transitional volcanism between the Sierra Madre Occidental and the Trans-Mexican Volcanic Belt. J Volcanol Geotherm Res 301:128–147

Graue B, Siegesmund S, Middendorf B (2011) Quality assessment of replacement stones for the Cologne Cathedral: mineralogical and petrophysical requirements. Environ Earth Sci 63:1799–1822

Griffith AA (1924) Theory of rupture. In: Proceedings of 1st international congress of applied mechanics. Delft, pp 55–63

Julia F, Vladimir L, Sergey R, David Z (2014) Effects of hydrothermal alterations on physical and mechanical properties of rocks in the Kuril–Kamchatka Island Arc. Eng Geol 183:80–95

Korkanç M (2013) Deterioration of different stones used in historical buildings within Nigde province, Cappadocia. Constr Build Mater 48:789–803
La Iglesia A, González V, López-Acevedo V, Viedma C (1997) Salt crystallization in porous construction materials I. Estimation of crystallization pressure. J Cryst Growth 177(1–2):111–118
La Russa MF, Ruffolo SA, Rovella N, Belfiore CM, Pogliani P, Pelosi C, Andaloro M, Crisci GM (2014) Cappadocian ignimbrite cave churches: stone degradation and conservation strategies. Periodico di Mineralogia 83(2):187–206
Leventis A, Verganelakis DA, Halse MR, Webber JB, Strange JH (2000) Capillary imbibition and pore characterization in cement pastes. Transp Porous Media 39:143–157
López-Doncel R, Wedekind W, Dohrmann R, Siegesmund S (2013) Moisture expansion associated to secondary porosity: an example of the Loseros Tuff of Guanajuato, Mexico. Envorin Earth Sci 69:1189–1201
López-Doncel R, Wedekind W, Leiser T, Molina-Maldonado S, Velasco-Sánchez A, Dohrmann R, Kral A, Wittenborn A, Aguillón-Robles A, Siegesmund S (2016) Salt bursting tests on volcanic tuff rocks from Mexico. Environ Earth Sci 69:1189–1201
López-Moreno A, Sepúlveda-Sánchez JD, Alonso Guzmán EM, Le Borgne S (2014) Calcium carbonate precipitation by heterotrophic bacteria isolated from biofilms forme don deteriorated ignimbrite Stones: influence of calcium on EPS production and biofilm formation by these isolates. Biofouling 30(5):547–560
Madsen FT, Müller-Vonmoos M (1989) The swelling behaviour of clays. Appl Clay Sci 4:143–156
Martínez-Martínez J, Benavente D, García-del-Cura MA (2011) Spatial attenuation: the most sensitive ultrasonic parameter for detecting petrographic features and decay processes in carbonate rocks. Eng Geol 119:84–95
Martínez-Martínez J, Benavente D, Gómez-Heras M, Marco-Castaño L, García-del-Cura MA (2013) Non-linear decay of building stones turing freeze–thaw weathering processes. Constr Build Mater 38:443–454
Mod'd BK, Howarth RJ, Bland CH (1996) Rapid prediction of building research establishment limestone durability class from porosity and saturation. Q J Eng Geol 29:285–297
Morales-Gámez M, Corona-Chávez P (2006) Geotecnia y problemática de extracción en los bancos de rocas ornamentales de la región de Tlalpujahua. Revista de Investigación de la Universidad Michoacana de San Nicolás de Hidalgo. 43:113–130
Ordóñez S, Fort R, García del Cura MA (1997) Pore size distribution and the durability of a porous limestone. Q J Eng Geol 30:221–230
Ostrooumov M (2009) A Raman IR and XRD análisis of the deterioration on historical monuments: case study from Mexico. Spectrochimica Acta Part A 73:498–504
Ostroumov M, Garduño-Monroy VH, Carreón-Nieto H, Lozano-Santa Cruz R (2003) Mineralogía y geoquímica de los procesos de degradación en monumentos históricos: primer acercamiento a un caso mexicano (Morelia, Michoacán). Revista Mexicana de Ciencias Geológicas 20(3):223–232
Özbek A (2014) Investigation of the effect of wetting–drying and freezing–thawing cycles on some physical and mechanical properties of selected ignimbrites. Bull Eng Geol Environ 73:595–609
Özvan A, Dinçer I, Akin M, Oyan V, Tapan M (2015) Experimental studies on ignimbrite and the effect of lichens and capillarity on the deterioration of Seljuk Gravestones. Eng Geol 185:81–95
Penide J, Quintero F, Riveiro A, Sánchez-Castillo A, Comesaña R, del Val J, Lusquiños F, Pou J (2013) Removal of graffiti from quarry stone by high power Diode laser. Opt Lasers Eng 51:364–370
Pereira D, Marker B (2016) The value of original natural stone in the context of architectural heritage. Geosciences 6:1–9
Pradal E, Robin C (1994) Long-lived magmatic phases at Los Azufres volcanic center, Mexico. J Volcanol Geotherm Res 63:201–215
Richardson BA (1991) The durability of porous stones. Stone Ind 26(10):22–25
Rodriguez-Navarro C, Dohene E (1999) Salt weathering: influence of evaporite rate, supersaturation and crystallisation pattern. Earth Surf Proc Land 23(3):191–209
Rozenbaum O, Barbanson L, Muller F, Bruand A (2008) Significance of a combined approach for replacement stones in the heritage buildings' conservation frame. C.R. Geoscience 340:345–355
Smith BJ, Gomez-Heras M, McCabe S (2008) Understanding the decay of stone-built cultural heritage. Prog Phys Geog 32(4):439–461
Smith BJ, Gomez-Heras M, Viles HA (2010) Underlying issues on the selection, use and conservation of building limestone. London: geological Society. Spec Publ 331:1–11
Topal T, Doyuran V (1998) Analyses of deterioration of the Cappadocian tuff, Turkey. Environ Geol 34:5–20
Topal T, Sözmen B (2003) Deterioration mechanisms of tuffs in Midas monument. Eng Geol 68:201–223
Ulusoy M (2007) Different igneous masonry blocks and salt crystal weathering rates in the architecture of historical city of Konya. Build Environ 42:3014–3024
UNE-EN 12370 (1999) Natural stone test methods. Determination of resistance to salt crystallisation. European Committee for Standarization, Madrid
UNE-EN 1925 (1999) Natural stone test method. Determination of water absorption coefficient by capillarity. European Committee for Standarization, Madrid
UNE-EN 1926 (2007) Natural stone test methods. Determination of uniaxial compressive strength. European Committee for Standarization, Madrid
UNE-EN (1936) Natural stone test method. Determination of real density and apparent density and of total and open porosity. European Committee for Standarization, Madrid
Urosevic M, Sebastián E, Cardell C (2013) An experimental study on the influence of surface finishing on the weathering of a building low-porous limestone in coastal environments. Eng Geol 154:131–141
Vergès-Belmin V (2010) Deterioration of stone in monuments. In: Schrefler B, Delage P (eds) Environmental geomechanics. ISTE Ltd, London
Wedekind W, López-Doncel R, Dohrmann R, Kocher M, Siegesmund S (2013) Weathering of volcanic tuff rocks caused by moisture expansion. Environ Earth Sci 69:1203–1224
Wellman HW, Wilson AT (1965) Salt weathering, a neglected geological erosive agent in coastal and arid environments. Nature 205:1097–1098
Yavuz AB (2012) Durability assessment of the Alacti tuff (Izmir) in western Turkey. Environ Earth Sci 67:1909–1925
Yavuz AB, Akal C, Türk N, Çolak M, Tanyu BF (2015) Investigation of discrepancy between tuff used as building stones in historical and modern buildings in western Turkey. Constr Build Mater 93:439–448
Yu S, Oguchi CT (2010) Role of pore size distribution in salt uptake, damage, and predicting salt susceptibility of eight types of Japanese building stones. Eng Geol 115:226–236
Zedef V, Kocak K, Doyen A, Ozsen H, Kekec B (2007) Effect of salt crystallization on stones of historical building and monuments, Konya, Central Turkey. Build Environ 42:1453–1457